

Gravitational waves from orbiting binaries without general relativity

Robert C. Hilborn

Citation: [American Journal of Physics](#) **86**, 186 (2018); doi: 10.1119/1.5020984

View online: <https://doi.org/10.1119/1.5020984>

View Table of Contents: <https://aapt.scitation.org/toc/ajp/86/3>

Published by the [American Association of Physics Teachers](#)

ARTICLES YOU MAY BE INTERESTED IN

[A study of kinetic friction: The Timoshenko oscillator](#)

American Journal of Physics **86**, 174 (2018); <https://doi.org/10.1119/1.5008862>

[Can mechanical energy vanish into thin air?](#)

American Journal of Physics **86**, 220 (2018); <https://doi.org/10.1119/1.5019022>

[The Toy model: Understanding the early universe](#)

American Journal of Physics **86**, 290 (2018); <https://doi.org/10.1119/1.5026694>

[The contrasting roles of Planck's constant in classical and quantum theories](#)

American Journal of Physics **86**, 280 (2018); <https://doi.org/10.1119/1.5021355>

[Double well potentials with a quantum moat barrier or a quantum wall barrier give rise to similar entangled wave functions](#)

American Journal of Physics **86**, 180 (2018); <https://doi.org/10.1119/1.5019166>

[Mass: The Quest to Understand Matter from Greek Atoms to Quantum Fields](#)

American Journal of Physics **86**, 237 (2018); <https://doi.org/10.1119/1.5021906>



Gravitational waves from orbiting binaries without general relativity

Robert C. Hilborn^{a)}

American Association of Physics Teachers, College Park, Maryland 20740

(Received 29 March 2017; accepted 26 December 2017)

Using analogies with electromagnetic radiation, we present a calculation of the properties of gravitational radiation emitted by orbiting binary objects. The calculation produces results that have the same dependence on the masses of the orbiting objects, the orbital frequency, and the mass separation as do the results from the linear version of general relativity (GR). However, the calculation yields polarization, angular distributions, and overall power results that differ from those of GR. Nevertheless, the calculation produces waveforms that are very similar to those observed by the Laser Interferometer Gravitational-Wave Observatory (LIGO-VIRGO) gravitational wave collaboration in 2015 up to the point at which the binary merger occurs. The details of the calculation should be understandable by upper-level physics students and physicists who are not experts in GR. © 2018 American Association of Physics Teachers.

<https://doi.org/10.1119/1.5020984>

I. INTRODUCTION

The recent observations^{1–4} of gravitational waves by the Laser Interferometer Gravitational-Wave Observatory (LIGO-VIRGO) collaboration have excited the physics community and the general public. The ability to detect directly gravitational waves provides a “new spectroscopy” that is likely to have a profound influence on our understanding of the structure and evolution of the universe and its constituents.

The LIGO-VIRGO collaboration provides strong evidence that the observed waves can be attributed to the inspiraling of two mutually orbiting black holes, ending with the coalescence of the black holes.⁵ To many physicists and certainly almost all students, the derivations of the expressions used to reveal the characteristics of the sources from the LIGO-VIRGO observations seem rather challenging due to the complicated formalism of general relativity (GR).

It is important to realize that almost any relativistic theory of gravity predicts the existence of gravitational waves traveling at a finite speed (Refs. 6, 7, and 8, pp. 242). In this paper, we provide a specific example of that claim. In fact, there were several attempts to build relativistic theories of gravity before Einstein published his version (general relativity) in 1915. Those involved include theories by Heaviside, Poincaré, Nordstrom and even Einstein himself. (For a summary of the history of those attempts, see Refs. 6, 7, and 9, Chap. 13.) All of those theories predicted the existence of gravitational waves though few worked out the detailed formalism. More recently, Schutz¹⁰ has presented a scalar field model of gravitational waves. In that model, the waves are longitudinal (rather than transverse).

In this paper, we treat the relationship between gravitational waves and their sources in analogy with the relationships for electromagnetic (E&M) waves, as a physicist might have done prior to 1915—after special relativity had been introduced but before Einstein formulated GR. It turns out that such a treatment produces most of the GR features of gravitational waves, but not all, as one might expect since GR is a tensor theory and electromagnetism is a vector theory. We hasten to point out that we are not constructing a complete relativistic theory of gravity.¹¹ To do so would require building in field energy as a source of gravitation, making the theory nonlinear. Our goals are more modest:

establishing the extent to which such a model can account for the production of gravitational waves from orbiting binaries and the detection of those waves far from their sources. As we shall see, the results of the calculations are in surprisingly good agreement with the LIGO-VIRGO observations and the calculations from numerical GR up to the time at which the binary objects “collide.” Of course, in hindsight we recognize that such an E&M-like theory, if it were to be constructed, is likely to give predictions for effects such as the advance of the perihelion of Mercury that differ from those of GR and certainly different predictions for behavior in very strong gravitational fields. Our hypothetical pre-1915 physicist, we assume, is interested only in the possibility of gravitational waves as observed far from their sources.

The arguments presented here should be readily accessible to physics faculty who are not experts in GR and to their upper-level undergraduate students. We have provided sufficient detail to keep the presentation self-contained. The effects of special relativity are included by using gravitational potentials that depend on the so-called retarded time relative to the observation time. The calculation reproduces most of the results obtained from the linear version^{8,12,13} of GR without invoking spacetime curvature or the energy-momentum tensor. In particular, the calculation shows “naturally” that gravitational waves are transverse and for an orbiting binary source, the radiated energy has the dependence on mass, orbital frequency, and mass separation predicted by linear GR. In addition to providing an accessible calculation of gravitational waves, the results will clarify which aspects of the LIGO-VIRGO observations require full-fledged GR and which can be accounted for in (almost) any relativistic theory of gravitational waves.

The strategy of the paper is the following:

- (1) Formulate the gravitational vector potential function due to the orbiting binary objects, taking into account the time delay between events at the binaries and measurements at the observation point.
- (2) Calculate the gravitational radiation field from the gravitational vector potential function.
- (3) Employ the gravitational radiation field to find the energy per unit time carried away from the binaries by gravitational waves.
- (4) Use Newtonian mechanics to determine how the orbits of the binary objects decay as they lose energy.

- (5) Combine the orbital dynamics with the energy loss to calculate the gravitational waveform and how that wave interacts with the LIGO-VIRGO detector to produce the observed signal.

II. ELECTROMAGNETIC WAVES PROVIDE A PARADIGM FOR GRAVITATIONAL WAVES

The analogy between electromagnetism (E&M) and gravitation makes use of the equivalent roles of $1/4\pi\epsilon_0$ (where ϵ_0 is the standard permittivity of free space) and G , the Newtonian gravitational parameter, when SI units are used in the expressions relating sources to potentials and fields. As in standard treatments of E&M, we focus on the use of scalar and vector potentials to take into account the finite propagation speed of “disturbances” in the fields via the retarded-time technique. The electric and magnetic fields themselves have a more complex dependence on the source properties than do the potentials (Ref. 14, pp. 422–423 and 427–428). The fields depend on both the charge density and current and their time derivatives.

First we review the description of electromagnetic waves and their relation to potential functions. As is well known, electric and magnetic fields can be expressed in terms of two potential functions:^{14,15} a scalar potential Φ and a vector potential \vec{A} . The electric and magnetic fields are found by calculating the space and time derivatives of the potential functions

$$\vec{E} = -\vec{\nabla}\Phi - \frac{\partial\vec{A}}{\partial t}, \quad (1)$$

$$\vec{B} = \vec{\nabla} \times \vec{A}. \quad (2)$$

In the so-called Lorenz gauge,¹⁶ (for which we invoke $\vec{\nabla} \cdot \vec{A} = -(1/c^2)\partial\Phi/\partial t$) the potential functions are given in terms of their sources (charges and currents) by

$$\vec{A}(\vec{R}, t) = \frac{\mu_0}{4\pi} \int \frac{\vec{J}(\vec{r}, t_r)}{|\vec{R} - \vec{r}(t_r)|} d^3r = \frac{\mu_0}{4\pi} \sum_i \frac{q_i \vec{v}_i(t_{r_i})}{|\vec{R} - \vec{r}_i(t_{r_i})|} \quad (3)$$

and

$$\begin{aligned} \Phi(\vec{R}, t) &= \frac{1}{4\pi\epsilon_0} \int \frac{\rho(\vec{r}, t_r)}{|\vec{R} - \vec{r}(t_r)|} d^3r \\ &= \frac{1}{4\pi\epsilon_0} \sum_i \frac{q_i}{|\vec{R} - \vec{r}_i(t_{r_i})|}, \end{aligned} \quad (4)$$

where the first set of source terms are integrals over a continuous current density (current per unit area) \vec{J} and continuous charge density (charge per unit volume) ρ . The second set of source terms are the appropriate forms for a collection of point particles whose charges do not change with time and whose speeds are small compared to the speed of light.¹⁷ In Eqs. (3) and (4), \vec{R} is the position vector of the observation point, \vec{r} is the position vector of the source point, the retarded time is given by $t_r = t - |\vec{R} - \vec{r}|/c$, and c is the wave propagation speed (assumed here to be the usual speed of light c). The retarded time in essence takes into account the time it takes the “message” to travel from the source point to the

observation point. In other words, what one observes at the observation point at time t is determined by what happened at the source at the earlier time t_r . Throughout this paper, we shall use upper-case (“large”) R to denote the distance between the source and a distant observer and lower-case (“small”) r to denote distances within the source.

To build a model of gravitational waves in analogy to the theory of electromagnetic waves, one simply replaces the “coupling constants” as follows:

$$\frac{1}{4\pi\epsilon_0} \rightarrow -G \text{ and equivalently } \frac{\mu_0}{4\pi} \rightarrow -\frac{G}{c^2}, \quad (5)$$

where μ_0 is the permeability of free space. In addition, charge is replaced with mass and electric current is replaced with mass current (mass flow per unit time). The minus signs are needed because the gravitational interaction between ordinary masses is always (as far as we know) attractive. Hence, the gravitational potential energy decreases as two “like” masses approach each other.

In analogy with E&M, we introduce gravitational scalar and vector potentials, which, in the Lorenz gauge satisfy the analogs of Eqs. (3) and (4). For a system of discrete masses, we have

$$\vec{A}_G(\vec{R}, t) = -\frac{G}{c^2} \sum_i \frac{m_i \vec{v}_i(t_{r_i})}{|\vec{R} - \vec{r}_i(t_{r_i})|}, \quad (6)$$

$$\Phi_G(\vec{R}, t) = -G \sum_i \frac{m_i}{|\vec{R} - \vec{r}_i(t_{r_i})|}, \quad (7)$$

where m is the mass and $m\vec{v}$ is the mass current, which is the equivalent of charge current density in E&M when the sources are discrete particles, as shown in Eq. (3). Each contribution to the right sides of Eqs. (6) and (7) is evaluated at the appropriate retarded time.

For the purposes of describing gravitational waves, which are transverse waves, it turns out to be expeditious to use the Coulomb gauge^{14–16,18} (for which we invoke $\vec{\nabla} \cdot \vec{A} = 0$) in place of the Lorenz gauge because in the Coulomb gauge the gravitational radiation field $\vec{E}_{G\text{rad}}$ depends only on the components of the vector potential $\vec{A}_{G\text{trans}}$ that are transverse to the observation direction

$$\vec{E}_{G\text{rad}} = -\frac{\partial \vec{A}_{G\text{trans}}}{\partial t} \equiv \vec{g}_{\text{rad}}. \quad (8)$$

Equation (8) introduces the familiar symbol \vec{g} to represent the local gravitational field. Here, we are concerned only with the time-dependent part describing gravitational radiation.

Note that Eq. (8) does not involve the scalar potential, in contrast to Eq. (1), which involves both the scalar and vector potentials. Of course, the physical fields should be independent of the choice of gauge. The details of the connections between the scalar and vector potentials in the Lorenz gauge and in the Coulomb gauge are discussed in detail by Brill and Goodman.¹⁹ The Coulomb gauge is convenient for our purposes because it allows us to focus entirely on the transverse components of the field.

The basic idea¹⁵ behind the Coulomb gauge is that the current can be separated into a longitudinal component (along the direction of observation) and a transverse component. It

turns out that the longitudinal current components are proportional to the gradient of the time derivative of the scalar potential. The crucial point is that in the Coulomb gauge, the scalar potential contributions fall off as the inverse square of the distance R between the source and observer while the radiation fields fall off only as $1/R$. Hence, at large distances from the source, the longitudinal current contributions can be ignored compared to the transverse components.

From Eq. (6), it turns out that the transverse components of the gravitational vector potential satisfy

$$\vec{A}_{G\text{trans}}(\vec{R}, t) = -\frac{G}{c^2} \left(\sum_i \frac{m_i \vec{v}_i(t_{r_i})}{|\vec{R} - \vec{r}_i(t_{r_i})|} \right)_{\text{trans}}. \quad (9)$$

In the SI system, the gravitational field \vec{g} calculated from Eqs. (8) and (9) has units of N/kg. In analogy with Eq. (2), we also expect to find a type of gravitational field akin to the magnetic field of E&M,

$$\vec{B}_G = \vec{\nabla} \times \vec{A}_G, \quad (10)$$

to which we shall return shortly.

For the analysis of gravitational waves emitted by orbiting binaries, we will need to find the energy carried away by the gravitational waves. To describe that energy, we again proceed in analogy with electromagnetism. In E&M, the power per unit area in the direction of wave propagation can be written as

$$S_{\text{EM}} = \frac{c}{2} \left(\epsilon_0 E^2 + \frac{1}{\mu_0} B^2 \right), \quad (11)$$

where S_{EM} is the magnitude of the electromagnetic Poynting vector.^{14,15} In practice, what one usually measures is the power averaged over several wave periods. (In E&M, the averaging is optional, but in GR it is essential because the localization of gravitational field energy is impossible.^{12,13,20}) With $|B| = |E|/c$ for E&M plane waves, the time-averaged Poynting vector for a wave traveling in the z direction can be expressed as

$$\langle \vec{S}_{\text{EM}} \rangle = c \epsilon_0 \langle \vec{E}^2(t) \rangle \hat{z}, \quad (12)$$

where the angular brackets indicate a time-average over several periods of oscillation. If the time dependence is sinusoidal, the averaging yields $\frac{1}{2}E^2$, where E is the amplitude of the oscillating field.

We assume that the power per unit area carried by a gravitational wave is given by expressions analogous to Eqs. (11) and (12) involving the time-average of a gravitational Poynting vector for a wave traveling in the z direction

$$\langle \vec{S}_G \rangle = \frac{c}{8\pi G} \langle \vec{g}_{\text{rad}}^2 + c^2 \vec{B}_{G\text{rad}}^2 \rangle \hat{z}. \quad (13)$$

Later we shall show that $|\vec{g}_{\text{rad}}|^2 = c^2 |\vec{B}_{G\text{rad}}|^2$ for monochromatic gravitational radiation fields far from their sources, so we may write the time-averaged gravitational Poynting vector as

$$\langle \vec{S}_G \rangle = \frac{c}{4\pi G} \langle \vec{g}_{\text{rad}}^2(t) \rangle \hat{z}. \quad (14)$$

Although this analogy seems straightforward, there are some subtleties associated with expressing gravitational field energy density both in the classical Newtonian formulation

and in general relativity.^{12,13,20} In particular, if we followed the substitution rules in Eq. (5), we would end up with negative energy carried by the gravitational radiation field. For now, we will ignore those issues and assume that disturbances (“wiggles”) in the gravitational field will cause oscillations of masses subject to that field and that hence the waves must carry positive energy.²¹

III. NEWTONIAN DYNAMICS FOR THE ORBITING BINARIES

To explain the recent observations of gravitational waves by the LIGO-VIRGO team,^{1,2,4} we will focus attention on the waves emitted by two masses orbiting their common center of mass. As mentioned previously, the LIGO-VIRGO observations are explained as detection of the gravitational waves emitted from the orbiting binaries during the decay of their orbits, that is, during the “inspiral” of the masses.

For simplicity’s sake, we will assume the orbits are circular in the absence of gravitational radiation and that when radiation is taken into account, the change in orbital properties is sufficiently slow that a circular orbit is still a reasonable model for the orbital dynamics over sufficiently small time steps. This assumption is violated in the last moments before the objects collide or merge, but nevertheless the circular orbit model provides a surprisingly good approximation.

For the geometry indicated in Fig. 1, the lower-case position vectors \vec{r}_a and \vec{r}_b give the positions of the masses relative to the center of mass, which we may assume to be at rest. (If we are moving relative to the center of mass, there will be, of course, a Doppler shift of the wave frequency.) The distance between the two masses is given by the sum of magnitudes $r = r_a + r_b$. We choose \vec{r} to be parallel to \vec{r}_a , so we may write

$$\vec{r}_a = \frac{m_b \vec{r}}{m_a + m_b} \quad \vec{r}_b = -\frac{m_a \vec{r}}{m_a + m_b}. \quad (15)$$

Assuming that Newtonian dynamics applies to the orbits (at least as a first approximation), we recognize that Newton’s second law for mass m_a requires that

$$F_{\text{on } a} = G \frac{m_a m_b}{r^2} = m_a \frac{v_a^2}{r_a}. \quad (16)$$

Invoking Eq. (15) and

$$v_a = \omega r_a, \quad (17)$$

where ω is the orbital frequency (in radians/s), yields

$$\omega^2 = G \frac{m_a + m_b}{r^3}, \quad (18)$$

which is Kepler’s third law for the binary system.

Ignoring for the moment any energy loss mechanisms, and introducing the retarded times

$$t_{Ra} = t - R_a/c \quad \text{and} \quad t_{Rb} = t - R_b/c, \quad (19)$$

we may write the position and velocity for mass m_a as

$$\vec{r}_a = r_a [\hat{x} \cos(\omega t_{Ra}) + \hat{y} \sin(\omega t_{Ra})] \quad (20)$$

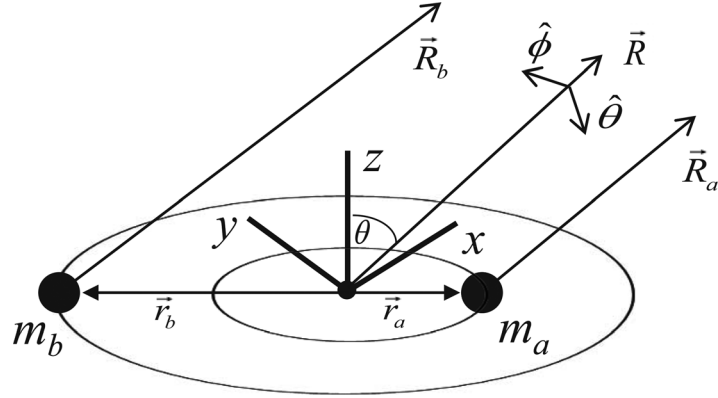


Fig. 1. A perspective view (from above and off to the side) of the geometry of the binary circular orbits. The x - y plane is chosen to coincide with the plane of the orbits. The distance between the two masses is given by $r = r_a + r_b$ and the vectors \vec{R}_a and \vec{R}_b point from mass m_a , and mass m_b , respectively, to the (distant) observation point. The vector \vec{R} points from the center of mass (small black dot) to the observation point. $\hat{\theta}$ and $\hat{\phi}$ are unit vectors perpendicular to \vec{R} . The x - y axes are aligned (without loss of generality because of the cylindrical symmetry around the z axis) so that $\vec{R} \cdot \hat{y} = 0$. The angle θ between the z axis and the observation direction is called the angle of inclination in the astrophysics literature.

$$\vec{v}_a = \omega r_a [-\hat{x} \sin(\omega t_{Ra}) + \hat{y} \cos(\omega t_{Ra})]. \quad (21)$$

The position and velocity for m_b are given by analogous expressions

$$\vec{r}_b = -r_b [\hat{x} \cos(\omega t_{Rb}) + \hat{y} \sin(\omega t_{Rb})], \quad (22)$$

$$\vec{v}_b = \omega r_b [\hat{x} \sin(\omega t_{Rb}) - \hat{y} \cos(\omega t_{Rb})]. \quad (23)$$

For later use, we will need

$$\vec{r} = r [\hat{x} \cos \omega t_R + \hat{y} \sin \omega t_R], \quad (24)$$

where $t_R = t - R/c$.

The total mechanical energy for the orbiting binaries is given by

$$U_{\text{total}} = \frac{1}{2} m_a v_a^2 + \frac{1}{2} m_b v_b^2 - G \frac{m_a m_b}{r} = -G \frac{m_a m_b}{2r}, \quad (25)$$

where the last equality follows from the use of Eqs. (17) and (18). As the system radiates gravitational wave energy, the mechanical energy of the binary system decreases (becomes more negative), which means that the distance between the two masses decreases, and by Eq. (18) the orbital frequency increases. It turns out that the energy carried away by a gravitational wave has a strong dependence on the orbital frequency, leading to a large increase in wave energy emitted as the distance between the masses decreases.

IV. VECTOR POTENTIAL FOR ORBITING BINARIES

The calculation of the gravitational vector potential, whose source is the sum of the mass currents associated with the system of two orbiting masses, will be guided by experience with E&M, as mentioned previously (see, for example, Ref. 14, Chap. 11). For a binary system of two point masses (objects whose spatial extent is very small compared to their separation), Eq. (9) becomes

$$\vec{A}_G(\vec{R}, t) = -\frac{G m_a \vec{v}_a(t_{Ra})}{c^2 R_a(t_{Ra})} - \frac{G m_b \vec{v}_b(t_{Rb})}{c^2 R_b(t_{Rb})}, \quad (26)$$

where the velocities and positions are evaluated at the appropriate retarded times.

We now take advantage of the fact that r_a and r_b are very small compared to R for any reasonable astrophysical situation. This fact will allow us to replace t_{Ra} and t_{Rb} in Eq. (26), with t_R plus small correction terms. To find those terms, we first express R_a in terms of R and r_a using the Law of Cosines

$$R_a = \sqrt{R^2 + r_a^2 - 2\vec{R} \cdot \vec{r}_a} = R \sqrt{1 - 2\frac{\vec{R} \cdot \vec{r}_a}{R^2} + (r_a/R)^2}. \quad (27)$$

Invoking $R \gg r_a, r_b$, introducing the unit vector $\hat{R} = \vec{R}/R$, and employing the binomial expansion yields

$$R_a \approx R - \hat{R} \cdot \vec{r}_a \quad \text{and} \quad R_b \approx R - \hat{R} \cdot \vec{r}_b, \quad (28)$$

keeping terms only through $\hat{R} \cdot \vec{r}_a$ and $\hat{R} \cdot \vec{r}_b$, which will be sufficient for the purposes of this calculation.

Let us now express the velocities in Eq. (26) in terms of the center of mass retarded time t_R plus small correction terms. To see how this works, we will use a Taylor series expansion of $\vec{v}_a(t - R_a/c)$ about the time $t - R/c$, that is, in powers of the difference

$$t - \frac{R_a}{c} - \left(t - \frac{R}{c} \right) = \frac{1}{c} (R - R_a) = \frac{1}{c} (\hat{R} \cdot \vec{r}_a) \equiv \Delta t_a, \quad (29)$$

where the penultimate equality in Eq. (29) follows from Eq. (28).

Using the standard Taylor series expansion formula yields

$$\vec{v}_a(t - R_a/c) = \vec{v}_a(t - R/c) + \frac{d\vec{v}_a}{dt} \Big|_{t-R/c} \Delta t_a + \dots \quad (30)$$

Equations (20) and (21) give

$$\frac{d\vec{v}_a}{dt} = -\omega^2 \vec{r}_a \quad (31)$$

with an analogous expression for the time derivative of \vec{v}_b .

Assembling these results and using $R \approx R_a \approx R_b$ in the denominator of Eq. (26) (all retarded time “corrections” in the denominator lead to terms that go as $1/R^2$, which we may ignore for radiation fields far from their sources), we find that the gravitational vector potential can be written as

$$\vec{A}_G(\vec{R}, t) = -\frac{G}{c^2 R} [m_a \vec{v}_a(t_R) + m_b \vec{v}_b(t_R)] + \frac{G\omega^2}{c^3 R} [m_a \vec{r}_a(\hat{R} \cdot \vec{r}_a) + m_b \vec{r}_b(\hat{R} \cdot \vec{r}_b)]. \quad (32)$$

In Eq. (32), all terms are evaluated at the same retarded time $t_R = t - R/c$. The first term on the right side of Eq. (32) vanishes because the net linear momentum of the orbiting binaries is zero. The remaining term goes as $1/R$, characteristic of a radiation field. For the E&M vector potential produced by two oppositely charged objects (an electric dipole), the corresponding first term does not vanish.

The second term involves products of the masses and the square of the distances from the center of mass, that is, they are related to the quadrupole moment tensor of the mass distribution $Q_{jk} = \sum_i m_i (3r_j r_k - r_i^2 \delta_{jk})$, where j and $k = x, y$, or z . This result indicates that gravitational radiation is primarily quadrupole (rather than dipole) radiation. Linear GR^{8,12,13} leads to the same conclusion.

Equation (32) can be put into a more transparent form by using Eq. (15) to replace \vec{r}_a and \vec{r}_b in favor of \vec{r}

$$\vec{A}_G(\vec{R}, t) = \frac{G\omega^2}{c^3 R} \frac{m_a m_b}{m_a + m_b} [\vec{r}(\hat{R} \cdot \vec{r}_a) - \vec{r}(\hat{R} \cdot \vec{r}_b)] = \frac{G\omega^2}{c^3 R} \eta M [\vec{r}(\hat{R} \cdot \vec{r})], \quad (33)$$

where the dimensionless mass ratio η is defined to be

$$\eta \equiv \frac{m_a m_b}{(m_a + m_b)^2}, \quad (34)$$

and the total mass is $M = m_a + m_b$. The combination ηM , the reduced mass of the system, will show up in many of our gravitational wave expressions. Please note that $\eta = 0.25$ for equal masses and is approximately equal to $m_{\text{small}}/m_{\text{large}}$ if one mass is much larger than the other.

We now use Eq. (24) to write the vector potential as

$$\begin{aligned} \vec{A}_G(\vec{R}, t) &= \frac{G\eta M \omega^2 r^2}{c^3 R} [(\hat{x} \cos \omega t_R + \hat{y} \sin \omega t_R) \\ &\quad \times (\hat{R} \cdot \hat{x} \cos \omega t_R)] \\ &= \frac{G\eta M \omega^2 r^2}{c^3 R} [\hat{x} \cos^2 \omega t_R + \hat{y} \cos \omega t_R \sin \omega t_R] \\ &\quad \times \hat{R} \cdot \hat{x} \\ &= \frac{G\eta M \omega^2 r^2}{2c^3 R} [\hat{x} (1 + \cos 2\omega t_R) + \hat{y} \sin 2\omega t_R] \\ &\quad \times \hat{R} \cdot \hat{x}. \end{aligned} \quad (35)$$

Note that the choice of the orientation of the x - y axes has eliminated $\hat{R} \cdot \hat{y}$ terms (see Fig. 1). The time-dependent terms indicate that the gravitational vector potential and hence the gravitational wave field oscillate with a frequency

which is twice the orbital frequency, a characteristic of quadrupole radiation from an orbiting binary system: after half an orbital period, the quadrupole moment returns to its initial value (since both x and y coordinates are reversed), indicating that the quadrupole moment oscillates with twice the orbital frequency.

To find the transverse components of the vector potential relative to the direction of observation, we express Eq. (35) in spherical coordinates (R, θ, ϕ) using the standard expressions

$$\begin{aligned} \hat{x} &= \sin \theta \cos \phi \hat{R} + \cos \theta \cos \phi \hat{\theta} - \sin \phi \hat{\phi} \\ &= \sin \theta \hat{R} + \cos \theta \hat{\theta}, \end{aligned} \quad (36)$$

$$\hat{y} = \sin \theta \sin \phi \hat{R} + \cos \theta \sin \phi \hat{\theta} + \cos \phi \hat{\phi} = \hat{\phi}, \quad (37)$$

$$\hat{R} \cdot \hat{x} = \sin \theta \cos \phi = \sin \theta. \quad (38)$$

The second equality in each of Eqs. (36)–(38) follows from the choice of $\phi = 0$ in the orientation of the x - y coordinate system relative to the observation direction. As mentioned previously, we will focus on just the $\hat{\theta}$ and $\hat{\phi}$ terms—the transverse terms.

Using the appropriate trigonometric relations to re-express the terms in Eq. (35) yields

$$\begin{aligned} \vec{A}_{G \text{ trans}} &= \frac{G\eta M \omega^2 r^2}{2c^3 R} \sin \theta \\ &\quad \times [\cos \theta (1 + \cos 2\omega t_R) \hat{\theta} + \sin 2\omega t_R \hat{\phi}]. \end{aligned} \quad (39)$$

We now take the time derivative of the transverse vector potential in Eq. (39) to get the gravitational radiation field

$$\begin{aligned} \vec{g}_{\text{rad}} &= -\frac{\partial \vec{A}_{G \text{ trans}}}{\partial t} \\ &= \frac{G\eta M \omega^3 r^2}{2c^3 R} [\sin 2\theta \sin 2\omega t_R \hat{\theta} - 2 \sin \theta \cos 2\omega t_R \hat{\phi}]. \end{aligned} \quad (40)$$

This is our fundamental result for the gravitational radiation field for the orbiting binaries. The Appendix describes how the same results are obtained in the Lorenz gauge.

Let us pause to make a general comment about the calculation: it is important to note that the use of “differential” retarded times in the analysis leads to expressions that depend on the structure of the source and the relative velocities of the source components. If we had evaluated Eq. (26) with only the retarded time associated with the center of mass $t_R = t - R/c$ and had ignored the differences in retarded times for the two masses, we would not have found any gravitational waves. The same comments apply to the importance of differential retarded time for E&M waves.¹⁴

It will be helpful in what follows to write Eq. (40) solely in terms of ω by using Kepler’s third law. We find that the gravitational radiation field can be expressed as

$$\begin{aligned} \vec{g}_{\text{rad}} &= \frac{\eta (GM)^{5/3} \omega^{5/3}}{2c^3 R} \\ &\quad \times [\sin 2\theta \sin 2\omega t_R \hat{\theta} - 2 \sin \theta \cos 2\omega t_R \hat{\phi}]. \end{aligned} \quad (41)$$

As the binary objects approach each other, the orbital frequency will increase and as Eq. (41) indicates, the amplitude will also increase. A signal that displays an increasing amplitude accompanied by an increasing frequency is called a “chirp.”

Our hypothetical pre-1915 physicist could use Eq. (41) to estimate the amplitude of the gravitational radiation field from a particular source. Obviously, we want to have large, nearly equal masses (to keep η as large as possible) orbiting at a high frequency and not too far away from Earth. The only obvious candidates in 1915 would be binary stars in the Milky Way. To see how the numbers work out, let’s assume that the sum of the masses is 20 solar masses and that the orbital separation between the stars is about the sum of their radii (estimated by scaling from the Sun’s radius). Let’s also assume that the binary stars are about 1000 light years away, well within the Milky Way. With those numbers we find that the orbital frequency ω is about 3×10^{-4} rad/sec and the amplitude of g_{rad} is about 10^{-16} N/kg. Such a small force per unit mass at such a low frequency would have discouraged almost anyone from thinking about detecting gravitational waves. But let’s continue with our analysis.

The field \vec{B}_G associated with the gravitational radiation is found from Eq. (39) by using the spherical coordinate form of the curl

$$\begin{aligned} \vec{\nabla} \times \vec{A} &= \frac{1}{r \sin \theta} \left[\frac{\partial}{\partial \theta} (\sin \theta A_\phi) - \frac{\partial A_\theta}{\partial \phi} \right] \hat{r} \\ &+ \frac{1}{r} \left[\frac{1}{\sin \theta} \frac{\partial A_r}{\partial \phi} - \frac{\partial}{\partial r} (r A_\phi) \right] \hat{\theta} \\ &+ \frac{1}{r} \left[\frac{\partial}{\partial r} (r A_\theta) - \frac{\partial A_r}{\partial \theta} \right] \hat{\phi}. \end{aligned} \quad (42)$$

Recalling that there is R dependence in the retarded time $t_R = t - R/c$, we see that derivatives with respect to R can be replaced by time derivatives using the standard chain rule

$$\frac{\partial f(t - R/c)}{\partial R} = -\frac{1}{c} \frac{\partial f}{\partial t}. \quad (43)$$

Using that result and dropping terms that go as $1/R^2$, we find

$$\vec{B}_{G\text{rad}} = \vec{\nabla} \times \vec{A}_G = \frac{1}{c} \left[(-g_{\text{rad}})_\phi \hat{\theta} + (g_{\text{rad}})_\theta \hat{\phi} \right]. \quad (44)$$

The important result is that $\vec{g}_{\text{rad}}^2 = c^2 \vec{B}_{G\text{rad}}^2$ just as $E^2 = c^2 B^2$ for E&M waves.

V. ENERGY CARRIED BY THE WAVES

We now want to find the time-average of the gravitational radiation Poynting vector, which expresses the power per unit area carried away by the gravitational wave. Using Eqs. (14) and (40) and straightforward algebra and trigonometry, we obtain

$$\begin{aligned} \langle S_G \rangle &= \frac{c}{4\pi G} \langle \vec{g}_{\text{rad}} \cdot \vec{g}_{\text{rad}} \rangle \\ &= \frac{G\omega^6(\eta M)^2 r^4}{32\pi c^5 R^2} [\sin^2 2\theta + 4 \sin^2 \theta], \end{aligned} \quad (45)$$

where we have made use of $\langle \cos^2 \omega t \rangle = \langle \sin^2 \omega t \rangle = 1/2$. We note that the angular distribution differs from that derived from the linear form of GR.^{8,12,13}

Finding the total gravitational power radiated requires that Eq. (45) be integrated over the surface of a sphere of radius R , centered on the source. In spherical coordinates the differential area on the surface of a sphere is given, as usual, by $R^2 \sin \theta d\theta d\phi$, so we need to integrate

$$\int_0^{2\pi} d\phi \int_0^\pi (\sin^2 2\theta + 4 \sin^2 \theta) \sin \theta d\theta = \frac{64\pi}{5}. \quad (46)$$

Assembling all of the results, we find that the total gravitational wave energy radiated per unit time can be written as

$$\frac{dE_G}{dt} = \frac{c}{32\pi G} \frac{G^2(\eta M)^2 r^4 \omega^6}{c^6} \frac{64\pi}{5} = \frac{2 G(\eta M)^2 r^4 \omega^6}{5 c^5}. \quad (47)$$

Equation (47) is the crucial result needed to account for the physics of the decay of the binary orbits. Except for the overall numerical factor, this result is in agreement with the result calculated from the linear version of GR.^{8,12,13} The GR numerical factor for the last term in Eq. (47) is $32/5$. The difference is attributable to the difference in angular distributions of the radiated power between the E&M-like model and linear GR results.

VI. THE BINARY INSPIRAL

As mentioned previously, the binary masses spiral in towards each other as gravitational waves carry energy away from the system. As a consequence, the orbital frequency increases. The increased orbital frequency leads to an increase in both the frequency and amplitude of the gravitational wave radiation field as described in Eq. (41). To see how the rate of change of the frequency $\dot{\omega}$ is related to the source properties, we construct an expression that indicates how the orbital frequency changes as the binary system radiates energy. We start by using the time derivative of Kepler’s third law, Eq. (18), to obtain

$$\dot{\omega} = -\frac{3}{2} \frac{\sqrt{GM}}{r^{5/2}} \dot{r}. \quad (48)$$

The time rate of change of r , the separation between the orbiting masses, can be related to the rate of change of orbital energy by combining Eq. (47), the energy loss expression (rewritten here with the numerical factor indicated by N)

$$\frac{dE_G}{dt} = N \frac{G(\eta M)^2 r^4 \omega^6}{c^5}, \quad (49)$$

with Eq. (25) to get

$$\dot{U}_{\text{total}} = \frac{Gm_a m_b}{2r^2} \dot{r} = -N \frac{G(\eta M)^2 r^4 \omega^6}{c^5}. \quad (50)$$

Again, using Kepler’s third law to replace ω in favor of r , we find

$$\dot{r} = -\frac{2NG^3 M m_a m_b}{c^5 r^3} = \frac{-2N(GM)^3 \eta}{c^5 r^3}, \quad (51)$$

which when combined with Eq. (48) gives

$$\dot{\omega} = \frac{3N\eta(GM)^{5/3}\omega^{11/3}}{c^5}. \quad (52)$$

Solving for $(\eta N)^{3/5}M$ yields

$$(\eta N)^{3/5}M = \frac{c^3}{3^{3/5}G} \left(\dot{\omega} \omega^{-11/3} \right)^{3/5}. \quad (53)$$

Note that Eq. (53) involves the so-called chirp mass $\eta^{3/5}M$.

Next we outline a method for calculating the binary mass separation as a function of time, given values of the masses, aiming for parameter values displaying the inspiral events inferred from the LIGO-VIRGO observations. Once we have found $r(t)$, we can use Kepler's third law to solve for $\omega(t)$.

First we note that the distance scale for any relativistic theory of gravity is set by the so-called Schwarzschild radius.²² The Schwarzschild radius can be defined as the distance from a mass M at which the escape speed is equal to the speed of light

$$r_S = \frac{2GM}{c^2}. \quad (54)$$

In what follows, we will use $M = m_a + m_b$ so that r_S is the sum of the Schwarzschild radii of the individual masses. It is interesting to note that the concept of an object whose gravity is sufficiently strong to prevent light from escaping from it was introduced in the 1700s independently by John Michell, an English clergyman and scientist, and Pierre-Simon Laplace, a French nobleman, mathematician and scientist.²³

Using Eq. (54) in Eq. (51), we find

$$\dot{r} = -2N\eta c \left(\frac{r_S}{r} \right)^3, \quad (55)$$

a remarkably simple expression. In essence, the Schwarzschild radius sets the scale for the inspiral. As $r \rightarrow r_S$, the rate of change of the separation increases dramatically. Note that for a given mass separation r , the E&M-like model ($N = 2/5$) gives a smaller rate of change of r than does the linear GR model ($N = 32/5$).

We can now calculate the orbits during the inspiral. First note that Eq. (55) may be integrated directly to find $r(t)$

$$r^4(t) = r_i^4 - N\eta r_S^3 c (t - t_i), \quad (56)$$

where r_i is the initial mass separation at time t_i . If r_i is a few times the Schwarzschild radius for the total mass, the inspiral will be easily noticeable. (Note that one could, alternatively, integrate Eq. (52) to find $\omega(t)$ and start the calculation based on an initial frequency rather than an initial mass separation.) Once we have $r(t)$ and $\omega(t)$, from Kepler's third law, we can easily find $v_{a,b} = \omega r_{a,b}$ to get the speeds of the masses relative to the center of mass.

The results of such a calculation are shown in Fig. 2 for $N = 32/5$ (the linear GR value) with $m_a = m_b = 35M_\odot$, where M_\odot is the mass of the Sun. The initial separation is $4.7r_S$. We see that strong orbit inspiral occurs over a period of only a few tenths of a second and the speed v of the masses relative to the center of mass is a few tenths of the

speed of light. From $\omega(t)$, we can calculate the gravitational radiation field from Eq. (41). A video simulation of the inspiraling binaries is available at the URL given in Ref. 24.

VII. APPLICATION TO THE LIGO-VIRGO INTERFEROMETERS

We now jump ahead from our pre-1915 scenario more than 100 years to see how to relate the oscillating gravitational field \vec{g}_{rad} to what the LIGO-VIRGO interferometers observe. GR brought the possibility of orbiting black holes with masses several times the solar mass acting as gravitational wave sources. That possibility and the tremendous advances in light sources, detectors, mirror coatings, and vacuum chamber and isolation engineering have made a reality of what our pre-1915 physicist would have viewed as almost impossible: direct detection of gravitational waves on Earth.

The LIGO-VIRGO observatory uses a relatively complex Michelson optical interferometer²⁵ with perpendicular arms of length L and Fabry-Perot cavities in each arm, to measure the “strain” $\Delta L/L$, where ΔL is the change in arm length induced by a gravitational wave. We will use a simple argument that relates \vec{g}_{rad} to $\Delta L/L$.

Interferometric gravitational wave detectors like LIGO-VIRGO respond to differential movements of parts of the apparatus (in particular, the interferometer mirrors and beam splitter in an interferometer arm). Differential movement occurs only if the gravitational wave interacts with the mirror and the beam splitter with (slightly) different phases.²⁶ In addition, the details relating the gravitational wave function \vec{g}_{rad} to the strain are complicated by the geometry of the wave propagation direction and polarization directions relative to the interferometer arms—the so-called antenna pattern. References 27 and 28 provide clear discussions of the interferometer antenna patterns for tensor (GR) gravitational waves. Reference 29 compares the antenna patterns for tensor (GR) waves and vector gravitational waves.

The antenna patterns for E&M-like gravitational waves are different from those for GR tensor waves for two reasons: (1) in GR the tensor polarization axes have an angle of 45° between them, whereas the E&M-like polarization basis vectors are perpendicular, and (2) the dependence on the angle of inclination of the binary orbit is different in the two models. As we have seen there is a $\sin \theta$ and $\sin 2\theta$

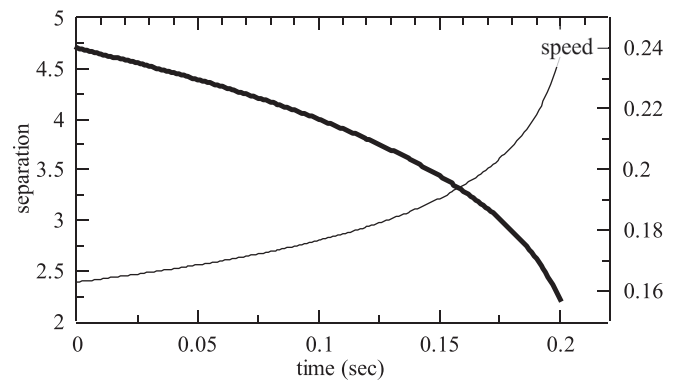


Fig. 2. The mass separation (thick curve, left axis in units of r_S , the sum of Schwarzschild radii of the two objects) and the speed (thin curve, right axis in units of c) of one of the masses relative to the center of mass of the system plotted as a function of time for the conditions stated in the text.

dependence in the E&M-like model as shown in Eq. (41), while linear GR has terms involving $\cos\theta$ and $(1 + \cos^2\theta)$.^{8,12,13}

In the simple model, the plane gravitational wave is propagating along the \hat{R} direction and we assume that the mirror and beam splitter are free to move only along \hat{x} (see Fig. 3). We assume that the polarization unit vector $\hat{\theta}$ is in the x - R plane and that $\hat{\phi} \cdot \hat{x} = 0$. In that case, we may use Eq. (41) to express the acceleration of mass 1 (the beam splitter) as

$$\ddot{x}_1 = \vec{g}_{\text{rad}} \cdot \hat{x} = \frac{\eta(GM)^{5/3}\omega^{5/3}}{2c^3R} \sin\beta \sin 2\theta \sin 2\omega t, \quad (57)$$

with a similar expression for mass 2 (the mirror).

Both the mirrors and the beam splitter in the LIGO-VIRGO interferometer are mounted as pendula²⁵ and are free to oscillate along the interferometer arm direction. The mirror and beam splitter can be modeled as linear, driven, damped oscillators. Since the gravitational wave frequency is much larger than the natural oscillation frequencies of the beam splitter and mirror pendula and since the damping is negligible during the time of interaction with the gravitational wave, we find that the displacements of the beam splitter and the mirror in the x direction are given approximately by

$$\Delta x(t) \approx -\frac{\vec{g}_{\text{rad}} \cdot \hat{x}}{(2\omega)^2}. \quad (58)$$

The minus sign in Eq. (58) simply tells us that the displacement and forcing term are π radians out of phase for the sinusoidal driving of an object at a frequency far above its natural oscillation frequency. The 2 in the denominator reminds us that the gravitational wave frequency is twice the binary orbital frequency.

From Eq. (58), we see that the differential movement of the beam splitter and the mirror depends on $\vec{g}_{\text{rad}}(t) - \vec{g}_{\text{rad}}(t - \Delta t)$, where $\Delta t = (R_2 - R_1)/c = L \cos\beta/c$. We should note that for the gravitational waves observed by LIGO-VIRGO, the gravitational wavelength is much larger than the length of the interferometer arms (about 4 km). That implies

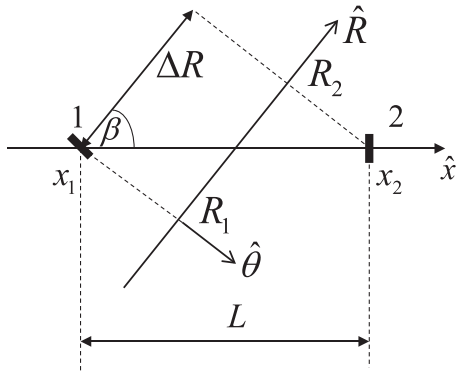


Fig. 3. The simple model for relative displacements of two masses, 1 (the beam splitter) and 2 (the mirror), in one arm of length L in the LIGO-VIRGO interferometer. The gravitational wave is traveling in the \hat{R} direction. The non-orthogonal (x, R) coordinates are given by (x_i, R_i) with $i = 1, 2$. $\hat{\theta}, \hat{x}, \hat{y}$ (not shown) and \hat{R} lie in the plane of the figure. We assume that the masses are free to move only in the x direction (along the interferometer arm). $\hat{\theta} \cdot \hat{x} = \sin\beta$, $\Delta R = R_2 - R_1$ and the length of the arm is given by $L = x_2 - x_1$.

that the time Δt for the wave to travel from the beam splitter to the mirror is much less than the period of the gravitational waves. Hence, we conclude that $\omega\Delta t \ll 1$ for the LIGO-VIRGO interferometers.

From Eqs. (57) and (58), we see that the time-dependent differential displacements of the two masses will be proportional to $\sin(2\omega t) - \sin(2\omega t - 2\omega\Delta t)$. Invoking $\omega\Delta t \ll 1$ and using standard trigonometry, we may write

$$\begin{aligned} \sin(2\omega t - 2\omega\Delta t) &= \sin(2\omega t) \cos(2\omega\Delta t) \\ &\quad - \cos(2\omega t) \sin(2\omega\Delta t) \\ &\approx \sin(2\omega t) - 2\omega\Delta t \cos(2\omega t). \end{aligned} \quad (59)$$

Assembling the results, we find that the fractional change in the arm length (the “strain”) in the x direction can be written as

$$\frac{\Delta L_x(t)}{L} = -\frac{\eta(GM)^{5/3}\omega^{2/3}}{c^4R} \cos(2\omega t) \times \text{angular factors.} \quad (60)$$

The differential motion in the y direction will have a similar form. Writing the combined angle-dependent factors as $F(\theta, \beta)$, we can then express the observed signal, which is proportional to the differences in strain in the two interferometer arms, as

$$\begin{aligned} h(t) &= \frac{\Delta L_x(t) - \Delta L_y(t)}{L} \\ &= -\frac{\eta(GM)^{5/3}\omega^{2/3}}{c^4R} F(\theta, \beta) \cos(2\omega t). \end{aligned} \quad (61)$$

Equation (61) provides the important information: The strain signal oscillates at twice the orbital frequency of the source and the amplitude depends on the combination $\eta M^{5/3}$ multiplied by $\omega^{2/3}$, exactly the dependence predicted by linear GR.^{8,12,13}

Using Kepler’s law to replace ω in Eq. (61) with r and introducing the Schwarzschild radius r_S , we find that the amplitude of the strain signal can be written in a simple form

$$|h(t)| = \frac{\eta r_S}{8r} \frac{r_S}{R} \times \text{angular factors.} \quad (62)$$

As we have noted previously, the Schwarzschild radius sets the distance scale for gravitational waves. The r_S/R factor shows how the amplitude falls off with distance from the source to the observation point and the r_S/r term tells us that the amplitude is largest when the mass separation approaches the combined Schwarzschild radii of the binary partners. If we can make reasonable estimates of the angular factors, we can use Eq. (62) and the measured amplitude of the strain signal to estimate the distance of the binaries from Earth (see Sec. VIII).

Results of this calculation are shown in Fig. 4, which plots the strain wave signal as a function of time for conditions close to those for the LIGO-VIRGO observations, described in detail in Sec. VIII. The signal consists of an oscillatory waveform with gradually increasing frequency and amplitude as the masses undergo an inspiral due to the loss of orbital energy to the emitted gravitational waves. Note that

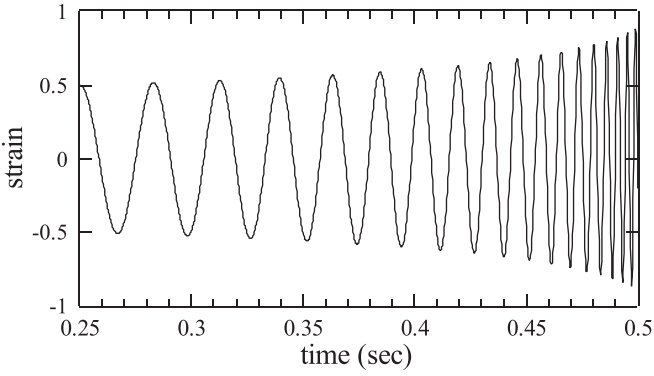


Fig. 4. The gravitational wave signal (arbitrary units) calculated from Eq. (61), plotted as a function of time with total mass $M = 65M_{\odot}$ and $\eta = 0.247$ (the LIGO-VIRGO results) with $N = 32/5$ for the linear GR theory, which is equivalent to $M = 340M_{\odot}$, $N = 2/5$, and $\eta = 0.25$ for the E&M-like model. Masses are multiples of the solar mass M_{\odot} . The initial value of the mass separation is $1.7r_{\text{s}}$ (1760 km) for the E&M-like model and $5.3r_{\text{s}}$ (1000 km) for the linear GR theory. The final value of the mass separation is $1.2r_{\text{s}}$ (1200 km) for the E&M-like model and $3.6r_{\text{s}}$ (680 km) for linear GR.

both the E&M-like model and linear GR give exactly the same waveform as long as the same $(\eta N)^{3/5}M$ is used in the two calculations.

VIII. COMPARISON TO THE LIGO-VIRGO DATA

Now we will compare the results of our calculations with the LIGO-VIRGO results for the GW150914 event (Gravitational Wave observed on September 14, 2015). The comparison of the E&M-like model calculations (and those from the linear form of GR) with the LIGO-VIRGO results is complicated by two factors. First, the LIGO observatory is sensitive only to gravitational waves with frequencies between approximately^{1,25} 35 and 350 Hz and the detection system contains moderately complex frequency filtering to reduce noise in the signal. Second, both the E&M-like model and the linear GR theory do not depend on and do not contain any information about the binary objects, whose internal structure becomes important when they “collide.” So, our analysis must be limited to comparing signals before the two objects merge and seeing what can be learned from the frequency of the waves and the frequency’s evolution with time.^{5,30,31} A summary of the full analysis using numerical GR for both the inspiral and the coalescence and the merger can be found in Ref. 32. A detailed review of the methods required to deal with the two-body problem in GR is given in Ref. 33. In what follows we will compare the results of the E&M-like model with the numerical GR results.

The LIGO-VIRGO collaborative web site³⁴ for the GW150914 event provides both the raw data for the observed waveforms and a numerical GR gravitational strain waveform corrected for the finite bandwidth of the instrument, frequency band rejection filters, and instrumental noise. Figure 5 shows the observed interferometer strain plotted as a function of time along with the predictions of numerical GR, including all the nonlinearities inherent in Einstein’s GR equation. The signal consists of an oscillatory part with gradually increasing frequency and amplitude as the binary masses approach each other. Then a sudden increase in the wave frequency and a rapid decay in amplitude at $t \approx 0.42$ s indicate the merger and coalescence of the two objects.

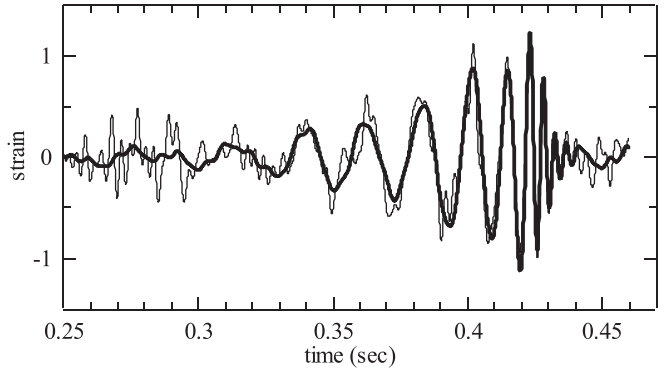


Fig. 5. The gravitational wave strain data (multiplied by 10^{21}) from the event GW150914 plotted as a function of time (in s). The thin curve is the raw data from the LIGO interferometer in Hanford, WA. The thick curve is the waveform from a full numerical GR calculation taking into account the frequency response of the detector system, see Ref. 1.

Let’s see how we might extract information from the waveform.^{5,30,31} Equation (53) indicates that the chirp mass $\eta^{3/5}M$ can be extracted from the data by finding $\omega(t)$ and $\dot{\omega}(t)$. From the LIGO-VIRGO data for GW150914 and using the linear GR value $N = 32/5$, we find the chirp mass is about $30M_{\odot}$. Assuming as a first approximation that the two masses are equal ($\eta = 1/4$), we find that the total mass is about $70M_{\odot}$. For the E&M-like model ($N = 2/5$), we find $M \approx 340M_{\odot}$. As mentioned previously, the waveforms from the two models agree exactly as long as the product $\eta^{3/5}MN^{3/5}$ is the same. However, different values of M will lead to different results for the mass separation $r(t)$.

Once we know the chirp mass, we could get an upper bound on the ratio of the two masses and hence rough approximations to the individual masses by requiring that the smallest separation of the masses, which occurs at the highest frequency of the signal, be larger than the sum of the Schwarzschild radii.⁵ However, at the smallest separations, the Newtonian description of the orbits certainly fails, so the estimates are relatively crude. The detailed numerical GR analysis, which includes information gleaned from the merger and ring-down, yields 36 and $29M_{\odot}$ (with uncertainties of about $5M_{\odot}$).

Once we have an initial estimate for the masses, we may calculate the gravitational wave strain signal using the method described previously. The results presented here were calculated using MATHEMATICA, but even a spreadsheet is adequate for the calculation. To match the LIGO-VIRGO numerical GR results for GW150914, we note that the initial wave frequency of the strain signal in Fig. 5 is about 30 Hz, corresponding to a wavelength of about 10^7 m, much larger than the LIGO-VIRGO interferometer arm length (about 4 km). We choose the initial separation of the two orbiting masses to give an orbital frequency $\omega/2\pi \approx 15$ Hz. The initial separation of the two masses is about 10^6 m for the LIGO-VIRGO masses and about 1.7×10^6 m for the E&M-like model mass values. Those separations are about a factor of 10 smaller than the emitted wavelength. So we see that the source is small compared to the emitted wavelength. The zero of time is adjusted to match the LIGO-VIRGO data.

The final separation is chosen so that the calculation matches the time in the LIGO-VIRGO signal at which “merger and ring-down” begins (at about 0.42 s in Fig. 5). That time corresponds approximately to the time at which the largest amplitude occurs.³⁵ For the purposes of this

paper, we plot the E&M-like model/linear GR waveform with an amplitude that is a multiple of the amplitude at $t = t_0$, where t_0 is the initial time point. Equation (61) tells us that the amplitude increases as $\omega^{2/3}$.

Figure 6 displays the results of the E&M-like model/linear GR theory along with the numerical GR results, the same as those plotted in Fig. 5 with the frequency filtering removed. The agreement is surprisingly good given that the E&M-like/linear GR models include none of the GR nonlinearities or relativistic dynamics effects. Those results match the numerical GR results except in the last few milliseconds, at which time the merger and ring-down occur. For the E&M-like calculation, the mass separation at about 0.42 s is $r \approx 1.37r_s \approx 1.4 \times 10^6$ m and $v/c \approx 0.3$ for each of the two masses. For linear GR, $r \approx 4.1r_s \approx 7.8 \times 10^5$ m and $v/c \approx 0.16$. Note that the final separation (about 10⁶ m) implies that the orbiting objects are most likely black holes, since of all known astronomical objects with masses on the order of 30–100 M_\odot , only black holes can approach that closely.^{5,35}

Since the product $\eta^{3/5}M$ occurs in both Eq. (52) and the strain signal Eq. (61), the data can also be used to estimate the distance from Earth to the binaries, if we make reasonable assumptions about the detector antenna pattern, the wave polarization and the binary orbit angle of inclination relative to the observing direction. The LIGO-VIRGO strain signal has an amplitude of about 10⁻²¹ for the GW150914 event and the full numerical GR analysis³⁵ yields a distance of about 410 Mpc [1 Megaparsec (Mpc) \approx 3.3 million light-years] with an uncertainty of about 170 Mpc. Using the E&M-like model and assuming that the values of each sine and cosine of the various angles in Eq. (61) are equal to 0.5, we find $R \approx 60$ Mpc. A smaller distance is consistent with the lower value of N and hence lower radiated power in the E&M-like model as compared to the linear GR theory.

The LIGO-VIRGO team estimated³⁵ that the GW150914 event had a peak gravitational luminosity of about 10⁴⁹ J/s. By way of comparison, the Sun's (electromagnetic) luminosity is about 10²⁶ J/s.

As an aside, we note that LIGO-VIRGO has two interferometer sites: one in Livingston, LA and the other in Hanford, WA. The comparison between the Hanford and Livingston signals allows estimates of the spatial location of the source in the sky since the signal arrived at Livingston

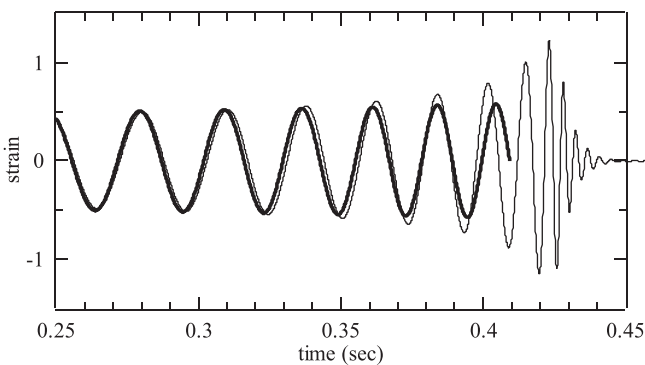


Fig. 6. The numerical GR calculation (without frequency filtering) of the LIGO-VIRGO strain signal (thin curve) (multiplied by 10²¹) plotted as a function of time for the GW150914 event, along with the predictions of the E&M-like model/linear GR model (thick curve) with parameters described in the text. The initial time was taken to match the LIGO-VIRGO plot. The initial wave frequency is 30.2 Hz. The ring-down and coalescence begin at about 0.42 s. The E&M-like model/linear GR calculation is stopped there.

about 6.9±0.5 ms before it arrived in Hanford,³⁵ in rough agreement with gravitational waves traveling at speed c over the approximately $D = 3000$ km “line of sight” (for gravitational waves) between Hanford and Livingston. Denoting the angle between the wave propagation direction and the line running from Livingston to Hanford as ϕ , we find that the time delay between the signals at the two detectors is given by $\Delta t = (D/c) \cos \phi$. For the GW150914 event, we obtain $\phi \approx 45^\circ$.

IX. DISCUSSION AND CONCLUSIONS

Using analogies with electromagnetism, we have seen that a relatively simple model of the gravitational radiation emitted by orbiting binaries reproduces many of the features of the linear GR calculations for the same system. The simple model does surprisingly well in describing the detected gravitational wave form observed by LIGO-VIRGO and the numerical GR calculations of those waveforms except for their final moments during which the merger and ring-down occur. The E&M-like model (as well as the linear GR model) is independent of the nature of the orbiting masses, so it can say nothing about what happens when the objects collide.

However, the polarization properties of the gravitational waves and the spatial distribution of the emitted energy and the overall numerical factor for the luminosity in the E&M-like model are notably different from the linear GR results.^{8,12,13} Although the physics underlying the two approaches is essentially the same (a time-dependent mass quadrupole moment leads to the emission of gravitational waves), the E&M-like model and GR handle the vector and tensor properties of the quadrupole moment somewhat differently, leading to differences in the angular distributions of emitted energy. In particular, for the circular binary orbit situation, Eq. (45) tells us that in the E&M-like model there is no gravitational radiation in the direction perpendicular to the plane of the binary orbit while linear GR^{8,12,13} predicts that the gravitational wave power is a maximum perpendicular to the plane of the orbit. There is, however, no information available about the orientation of the binary orbits for the recent LIGO-VIRGO observations. Also, the E&M-like model predicts two orthogonal polarizations with a $\pi/2$ temporal phase shift between them while GR gives two tensor polarizations whose axes are 45° apart with the same $\pi/2$ temporal phase shift between them.³⁶

For short (a few tenths of a second) gravitational wave events such as GW150914, the angular factors are essentially constant. However, if the detector system observes gravitational waves from sources that produce approximately continuous periodic waves, the relative orientation of the interferometer and the wave propagation direction and wave polarization would vary smoothly over a daily cycle and that modulation would provide detailed information about the polarization of the gravitational waves.

For short duration gravitational wave events, the difference in the polarization properties of the gravitational waves between GR and the E&M-like model, as well as in other alternative theories of gravitation,²⁹ can in principle be tested once additional gravitational wave observatories are active on Earth. Those other observatories will be oriented differently relative to the gravitational wave propagation direction so that comparing data among the observatories should yield information about the wave polarization.^{37,38}

For the sake of completeness, we point out another set of observations that indicate the existence of gravitational waves. The detailed timing measurements of the radio-frequency pulses emitted by the Taylor-Hulse binary pulsar³⁹ over several decades of observations indicate that the orbital period of the pulsar is decreasing at a rate completely consistent with the orbital energy loss due to gravitational waves predicted by linear GR (Eq. (47) with the linear GR factor of 32/5). This result seems to rule in favor of the linear GR approach. We note that the pulsar orbital period decay rate is 10^{11} times smaller than the decay rate observed in the black hole inspiral observed by LIGO-VIRGO. The E&M-like model analysis of the pulsar orbital period decay rate will be discussed in a separate publication.

Our pre-1915 physicist would probably be surprised that the E&M-like calculation does as well as it does, given the differences between GR and the pre-1915 model. The important “take home message” from this paper is that GR, although it is our most fully tested relativistic theory of gravitation, is not needed to give reasonable accounts of many of the properties of the recent direct detection of gravitational waves. This comment should not be taken as down-playing the revolutionary way of thinking about gravitation that is embodied in GR. As mentioned previously, accounting for the details of the source behavior as the binary objects coalesce does require GR (in the case of two black holes) or other detailed astrophysics for the case of colliding neutron stars,³⁸ for example.

The results presented here should encourage us to temper some of the rhetoric surrounding the first observations of gravitational waves.⁴⁰ Many writers claim that only GR predicts gravitational waves. As we noted previously, almost any relativistic theory of gravitational interactions will predict the existence of gravitational waves. This paper provides a concrete realization of that statement and we have shown that the E&M-like model can explain many of the experimentally observed properties of gravitational waves.

MATHEMATICA notebooks and an Excel spreadsheet for carrying out the calculations and a GlowScript simulation of the inspiral are available upon request from the author. A tutorial form of this paper directed at students is available at arXiv: 1710.04635.

ACKNOWLEDGMENTS

Thomas A. Moore, Joseph C. Amato, Hongbin Kim, and James Battat provided invaluable and much appreciated comments on both the content and style of draft versions of this paper. The author also thanks three anonymous reviewers for their many helpful comments. This research has made use of data, software and/or web tools obtained from the LIGO Open Science Center (<https://losc.ligo.org>), a service of LIGO Laboratory and the LIGO Scientific Collaboration. LIGO is funded by the U.S. National Science Foundation.

APPENDIX: LORENZ GAUGE CALCULATIONS

In this appendix, we give a brief outline of how one could arrive at Eq. (40) for the gravitational radiation field using the Lorenz gauge in place of the Coulomb gauge. For the Lorenz gauge calculation, we need to include the scalar

potential Φ_G and the longitudinal component of the vector potential (that is, the component along the observation direction \hat{R}), both of which we ignored in the Coulomb gauge calculation.

The calculation proceeds in close analogy with that given in the main part of this paper. For the contribution from the scalar potential, we find after a relatively lengthy calculation that

$$\bar{g}_{\text{rad}}^{(\Phi)} = -\frac{\eta GM\omega^3 r^2}{Rc^3} \sin^2\theta \sin 2\omega t \hat{R}. \quad (\text{A1})$$

Similarly, the longitudinal component from the vector potential is

$$\bar{g}_{\text{rad}}^{(A)} = +\frac{\eta GM\omega^3 r^2}{Rc^3} \sin^2\theta \sin 2\omega t \hat{R}. \quad (\text{A2})$$

We see that the two longitudinal components cancel and we are left with only the transverse components as expected. It is interesting to note that the same cancellation of longitudinal components occurs in the calculation of the electric field in dipole radiation, see Ref. 14, p. 447.

^{a)}Electronic mail: rhilborn@aapt.org

¹B. P. Abbott *et al.*, “Observation of gravitational waves from a binary black hole merger,” *Phys. Rev. Lett.* **116**, 061102 (2016).

²B. P. Abbott *et al.*, “GW151226: Observation of gravitational waves from a 22-solar-mass binary black hole coalescence,” *Phys. Rev. Lett.* **116**, 241103 (2016).

³Don Lincoln and Amber Stuver, “Ripples in reality,” *Phys. Teach.* **54**, 398–403 (2016).

⁴B. P. Abbott *et al.*, “GW170104: Observation of a 50-solar-mass binary black hole coalescence at redshift 0.2,” *Phys. Rev. Lett.* **118**, 221101 (2017).

⁵LIGO Scientific and VIRGO Collaborations, “The basic physics of the binary black hole merger GW150914,” *Ann. Phys.* **529**, 1600209 (2017).

⁶Daniel Kennefick, “Controversies in the history of the radiation reaction problem in general relativity,” e-print [arXiv:gr-qc/97040021-33](https://arxiv.org/abs/gr-qc/97040021) (1997).

⁷Daniel Kennefick, *Traveling at the Speed of Thought: Einstein and the Quest for Gravitational Waves* (Princeton U.P., Princeton, 2007).

⁸Hans Ohanian and Remo Ruffini, *Gravitation and Spacetime*, 2nd ed. (W. W. Norton & Company, New York, 1994).

⁹Abraham Pais, *Subtle is the Lord: The Science and the Life of Albert Einstein* (Oxford U.P., New York, 1982).

¹⁰Bernard F. Schutz, “Gravitational waves on the back of an envelope,” *Am. J. Phys.* **52**, 412–419 (1984).

¹¹Carver Mead, “Gravitational waves in G4v,” e-print [arXiv:gr-qc/1503.04866v1](https://arxiv.org/abs/gr-qc/1503.04866v1) (2015).

¹²C. Misner, K. Thorne, and J. A. Wheeler, *Gravitation* (W. H. Freeman, New York, 1973).

¹³Thomas A. Moore, *A General Relativity Workbook* (University Science Books, Mill Valley, California, 2013).

¹⁴David J. Griffiths, *Introduction to Electrodynamics*, 4th ed. (Pearson-Addison-Wesley, New York, 2012).

¹⁵J. D. Jackson, *Classical Electrodynamics*, 2nd ed. (John Wiley & Sons, New York, 1975).

¹⁶J. D. Jackson and L. B. Okun, “Historical roots of gauge invariance,” *Rev. Mod. Phys.* **73**, 663–680 (2001).

¹⁷The second set of terms in Eqs. (3) and (4) are the non-relativistic versions of the well-known Liénard-Wiechert potentials for point charges. The relativistic versions have a factor of $1 - R \cdot \vec{v}/c$ in the denominator.

¹⁸One can also use the Liénard -Wiechert potentials, Eqs. (3) and (4), with the relativistic “correction” in the denominators. That procedure gives the same results as those derived in this paper, but with a bit more algebra.

¹⁹O. L. Brill and B. Goodman, “Causality in the Coulomb gauge,” *Am. J. Phys.* **35**, 832–837 (1967).

²⁰P. C. Peters, “Where is the energy stored in a gravitational field?,” *Am. J. Phys.* **49**, 564–569 (1981).

- ²¹Reference 7 describes the history of this argument originally developed by Bondi and Pirani. The most famous version is due to Feynman and is called the “sticky bead argument.” <https://en.wikipedia.org/wiki/Sticky_bead_argument>.
- ²²Using the term Schwarzschild radius violates our pre-1915 scenario since Schwarzschild did not publish his solution of Einstein’s equation for static, spherically symmetric mass distributions until 1916.
- ²³Colin Montgomery, Wayne Orchiston, and Ian Whittingham, “Michell, Laplace, and the origin of the black hole concept,” *J. Astron. Hist. Herit.* **12**, 90–96 (2009).
- ²⁴A video simulation of two black holes merging can be found at <<https://apod.nasa.gov/apod/ap160212.html>>.
- ²⁵LIGO Scientific Collaboration, “Advanced LIGO,” e-print [arXiv:1411.4547](https://arxiv.org/abs/1411.4547) (2014).
- ²⁶Peter R. Saulson, “If light waves are stretched by gravitational waves, how can we use light as a ruler to detect gravitational waves?,” *Am. J. Phys.* **65**, 501–505 (1997).
- ²⁷Robert L. Forward, “Wideband laser-interferometer gravitational-radiation experiment,” *Phys. Rev. D* **17**, 379–390 (1978).
- ²⁸Atsushi Nishizawa, Atsushi Taruya, Kazuhiro Hayama, Seiji Kawamura, and Masa-aki Sakagami, “Probing non-tensorial polarization of stochastic gravitational-wave backgrounds with ground-based laser interferometers,” *Phys. Rev. D* **79**, 082002 (2009).
- ²⁹Maximiliano Isi, Alan J. Weinstein, Carver Mead, and Matthew Pitkin, “Detecting beyond-Einstein polarizations of continuous gravitational waves,” *Phys. Rev. D* **91**, 082002 (2015).
- ³⁰Louis J. Rubbo, Shane L. Larson, Michelle B. Larson, and Dale R. Ingram, “Hands-on gravitational wave astronomy: Extracting astrophysical information from simulated signals,” *Am. J. Phys.* **75**, 597–601 (2007).
- ³¹J. Amato, *Physics From Planet Earth: Gravitational Radiation* 2; available at <<https://physicsfromplanetearth.wordpress.com/2016/05/>>. Accessed August 29, 2017.
- ³²John G. Baker, Joan Centrella, Dae-II Choi, Michael Koppitz, and James van Meter, “Gravitational-wave extraction from an inspiralling configuration of merging black holes,” *Phys. Rev. Lett.* **96**, 111102 (2006).
- ³³Thibault Damour, *Frontiers in Relativistic Celestial Mechanics, Theory*, Sergei M. Kopeikin, editor (de Gruyter, Berlin, 2014) Vol. 1, pp. 1–38.
- ³⁴The LIGO Open Science Center URL is <<https://losc.ligo.org/>>.
- ³⁵B. P. Abbott *et al.*, “Properties of the binary black hole merger GW150914,” *Phys. Rev. Lett.* **116**, 241102 (2016).
- ³⁶Richard H. Price, “General relativity primer,” *Am. J. Phys.* **50**, 300–329 (1982).
- ³⁷B. P. Abbot *et al.*, “GW170814: A three-detector observation of gravitational waves from a binary black hole coalescence,” *Phys. Rev. Lett.* **119**, 141101 (2017).
- ³⁸B. P. Abbott *et al.*, “GW170817: Observation of gravitational waves from a binary neutron star inspiral,” *Phys. Rev. Lett.* **119**, 161101 (2017).
- ³⁹J. M. Weisberg, D. J. Nice, and J. H. Taylor, “Timing measurements of the relativistic binary pulsar PSR B1913+16,” *Astrophys. J.* **722**, 1030–1034 (2010).
- ⁴⁰Adrian Cho, “The cosmos aquiver,” *Science* **354**, 1516–1517 (2017).



Dynamometer

How do you measure a fairly large force? One technique is to use a helical spring, hung up vertically with a series of known weights hung from the bottom to calibrate it. If you do not exceed certain limits, the extension of the spring is linear with respect to the applied force. An alternative is the dynamometer, invented by Edmund Regnier and described by him in 1798. The dial scale indicated the increase in length of the pair of linked steel bars. This example is at Cornell University. (Picture and Notes by Thomas B. Greenslade, Jr., Kenyon College)